Toxicology 519 (2026) 154299

Contents lists available at ScienceDirect

Toxicology

journal homepage: www.elsevier.com/locate/toxicol

Particulate matter extracted from human anthracotic tissues induces inflammatory markers in co-culture of lung cells and macrophages

Daniela Perroni Frias [a,1,*], Gabriela Lima Vieira [a], Juliana Smelan [a], João Paulo Amorim De Lacerda [b], Paulo Sergio Cardoso da Silva [c], Fábio Vitório Sussa [c], Regiani Carvalho-Oliveira [a], Paulo Hilário Nascimento Saldiva [d], Thais Mauad [d], Mariangela Macchione [a]

[a] Laboratory of Experimental Environmental Pathology, School of Medicine, University of São Paulo, São Paulo, SP, Brazil
[b] Laboratory of Chemistry and Manufactured Goods, Institute of Technological Research, São Paulo, SP, Brazil
[c] Research Reactor Center – Nuclear and Energy Research Institute (IPEN), São Paulo, Brazil
[d] Department of Pathology, Faculty of Medicine, University of São Paulo, São Paulo, SP, Brazil

ARTICLE INFO

Keywords:
Anthracosis
Air pollution
CYP450
Polycyclic Aromatic Hydrocarbons
Macrophages
Inflammation

ABSTRACT

Anthracosis, characterized by black pigmentation in the lungs and tracheobronchial tree due to inhaled carbon particles, has been linked to urban air pollution. This study analyzed the chemical composition of particulate matter extracted from anthracotic tissue (APE) and its effects on human bronchial cells (BEAS-2B) and lung adenocarcinoma cells (A549) in co-culture with M1 or M2 macrophages. Diesel exhaust particles (DEP) served as a positive control. APE was extracted from lung and lymph nodes at Capital Death Verification Service (SVO) and chemically characterized for polycyclic aromatic hydrocarbons (PAHs) and inorganic elements like metals and sulfur. DEP contained more complex PAHs and higher levels of iron, sulfur, and zinc than APE. Pulmonary cell's metabolism decreased after exposure to APE, also co-culture macrophage viability. Macrophage immunophenotyping revealed heterogeneity, with M1 and M2 markers present in mono- and co-cultures, but APE exposure induced a pro-inflammatory M1 profile. Cytokine analysis showed significant increases in IL-1β, TNF-α, IL-6, and IL-8 levels after APE exposure, but not DEP. Gene expression of CYP1A1 and CYP1B1, associated with xenobiotic responses, increased after DEP exposure but remained unaffected by APE. Both APE and DEP caused mild modulation of cell cycle markers p53 and EGFR. These findings suggest APE is a metabolized particle, but not inert, inducing a pro-inflammatory response in pulmonary cells. Differences between APE and DEP effects likely stem from compositional variations: DEP's higher PAHs amount elicited a xenobiotic response, whereas APE's lower-weight PAHs triggered pronounced cytokine release.

1. Introduction

Anthracosis is a condition characterized by the black pigmentation of lungs and tracheobronchial tree caused by the deposition of inhaled carbon particles. Tissue pigmentation is derived from endocytosed carbon particles and occurs in lungs and lymph nodes (Mirsadraee, 2014; Jamaati et al., 2017a). With the first industrial revolution the use of coal increased the amount of smoke and particulate matter in cities, drawing the attention of scientists to a condition of intense lung pigmentation in coal miners, which led to the use of the term anthracosis for the first time (Klotz, 1914). Since then, anthracosis is generally related to occupational exposure of coal workers and miners, domestic exposure to biomass in rural areas of developing countries (Mirsadraee, 2014; Jamaati et al., 2017a), smokers (Hou et al., 2021) and populations in large urban areas with high levels of air pollutants (Kim et al., 2009; Törün et al., 2007; Boonsarngsuk et al., 2009).

Particles deposited in the pulmonary region may remain for months, years or indefinitely in various interstitial sites (Watson and Bates, 1988; Darquenne, 2020; Clarà et al., 2023; Kampa and Castanas, 2008; Leikauf et al., 2020). Macrophages might play a central role in lung particle accumulation, since the amounts of phagocytized particles depends on the amount of inhaled particulate matter (PM) and time of exposure to

* Corresponding author.
E-mail address: danielapfrias@alumni.usp.br (D.P. Frias).
[1] Present address: Karolinska Institutet - Institutet för miljömedicin, Unit of Biochemical Toxicology, Stockholm - Sweden.

https://doi.org/10.1016/j.tox.2025.154299
Received 25 August 2025; Received in revised form 2 October 2025; Accepted 6 October 2025
Available online 6 October 2025

air pollution (Bai et al., 2018; Kulkarni et al., 2006). It has been shown that the number of phagocytes found within the alveoli is proportional to the quantity of pigment in the pulmonary alveolus, while the quantity of pigment increases with advancing age (Klotz, 1914).

A research conducted in Guarulhos, metropolitan region of São Paulo, found that non-smoking residents who live in air polluted area had a greater amount of carbon pigment in their tracheobronchial wall when compared to non-smoking residents of less air polluted cities, evidencing that anthracosis may represent a marker of exposure to air pollution (Souza et al., 1998). In a carried out autopsy-based study with residents of the city of São Paulo, the proportion of anthracosis on the pleural surface of the lungs was positively associated with age and exposure to traffic-derived polluted air, suggesting a time-dependent pattern (Takano et al., 2019).

Although frequently observed in the lungs, the chemical characteristics and possible biological effects of particulate matter in anthracotic tissue have been rarely studied. Known data come from PM extracted from environmental sources presented mainly carbonaceous particles with adsorbed substances, as reactive metals like iron, copper, nickel, zinc, and vanadium; volatile organic compounds, as polycyclic aromatic hydrocarbons (PAHs); ions in nitrates and sulfates forms; and other materials of biologic and mineral origins (Kampa and Castanas, 2008; Hamanaka and Mutlu, 2018; Valavanidis et al., 2008).

There are several biological effects related to PM exposure such as oxidative stress by oxygen-free radicals' generation, causing DNA and cellular membrane oxidative damage, contributing to occurrence of respiratory infections, chronic cardiopulmonary diseases and increased lung cancer risk (Valavanidis et al., 2008). Also, PM exposure induces inflammatory cytokines release, such as IL-6, IL-8, and TNF-α, from both immune and structural airway cells (Leikauf et al., 2020). However, the potential adverse effects of accumulation are not clearly understood.

Experimental studies demonstrated that chronic exposure to PM results in a significant increase in expression of cancer related genes (Hu et al., 2017) with increased expression of tumor suppressors genes in the initial stage of exposure, followed by decreased expression in intermediate and late stages, indicating possible inactivation of tumor suppressors after prolonged exposure (Cui et al., 2019). PAHs are one of the main compounds in PM related to oxidative stress, inflammation and are considered procarcinogens because their metabolism within cells generates carcinogenic metabolites, which contribute to the etiology of cancer (Moorthy et al., 2015). Their transformation involves several enzymes, such as the cytochrome P450 family (CYPs) (Moorthy et al., 2015).

Malignant lesions associated with anthracosis have been sparsely reported (Mirsadraee, 2014). Biopsy studies showed increased oncogenes expression and lower tumor suppressor expression in the center of anthracotic lesions compared to margins (Jamaati et al., 2017b), while relatively advanced and less-differentiated adenocarcinomas tended to develop in severely anthracotic lungs (Wang et al., 2003).

There is no data on the chemical composition of the anthracotic pigment accumulated in the lungs of individuals living in urban areas and exposed to air pollution. During PM inhalation, phagocytosis and internalization, several biochemical processes may transform its composition. If they have already been metabolized and enclosed by macrophages, are they still capable of causing harm? Or do they retain chemical substances – such as metals and PAHs – in amounts that could lead to prolonged tissue damage? Chronic accumulation of anthracotic pigment may therefore induce different biological responses related to inflammation and cancer.

Therefore, the aim of this study was to chemically characterize anthracosis extracted from the lung, pleura and lymph nodes and verify its biological effects in a co-culture model of pulmonary cells and macrophages.

2. Methods

This study was approved by the Research Ethics Committee of the School of Medicine of São Paulo University under registration PB #08304519.4.0000.0065.

2.1. Particles

Two types of particles were used: particulate matter extracted from anthracotic lungs, the main focus of the study, and diesel exhaust particles, used as a positive control for anthracosis.

2.2. Anthracotic tissue collection

The extract of anthracosis particulate matter used in this study was collected from patients undergoing coroner autopsy at the São Paulo Death Verification Service, at the School of Medicine of São Paulo University. We collected tissue samples of lungs and mediastinal lymph nodes from individuals that lived in the metropolitan region of São Paulo for at least 5 years. Collections were conducted from August 2019 to October 2019. There was written informed consent from the next-of-kin in all cases.

2.3. Extraction of anthracotic tissue particulate matter (APE)

2.3.1. Lung digestion

The protocol for APE extraction was adapted from Catarino et al. and Amato-Lourenço et al. Fragments of lymph nodes and lungs were weighed, chopped, and remained under agitation overnight in a solution of 1.5 mL Corolase 7089 (AB Enzymes™) in 100 mL MilliQ water. The system was heated to 60°C for 24 h, as shown in Supplementary Information (SI) Figure 1. Corolase 7089 is used for the hydrolysis of proteins from several animal and plant sources, according to manufacturer information.

2.3.2. Washing and lyophilization

After the digestion of the biological material, the resulting liquid phase was washed by cycles of centrifugation and resuspension, using PBS or culture medium, resulting in black precipitate. Details of washing steps can be found in SI. After 4 h in the lyophilizer, the samples were in powder form and were stored in a desiccator. The total weight of the collected lung and lymph node fragments was 141.55 g, and the weight of the black powder obtained at the end of digestion was 797.3 mg (SI Figure 2).

2.4. Diesel exhaust particles (DEP)

Diesel Exhaust Particles (DEP) were chosen as a control for this study, as they are part of urban air pollution and are known to cause adverse biological effects. They were collected directly from a diesel engine using a particle trap attached to the vehicle's exhaust, i.e., there was no interaction with atmospheric substances or individuals. (Frias et al., 2020). DEP was kept in a dark glass container, at 4ºC.

2.5. Decontamination

Decontamination of APE and DEP was carried out by Cobalt 60 gamma irradiation, using the GAMMACELL apparatus (IPEN – Institute for Energy and Nuclear Research – University of São Paulo), with a dose of 25 KiloGrays for 72 h (Nguyen et al., 2007). After decontamination, the particles were stored in liquid nitrogen at approximately −120°C.

2.6. Particle characterization

2.6.1. Organic compounds

The determination of Polycyclic Aromatic Hydrocarbons (PAHs) was carried out at the Laboratory of Chemistry and Manufactured/ Bio-nanomanufacturing of the Institute of Technological Research – IPT, São Paulo, SP. The particles were characterized before and after the process of decontamination.

Approximately 100 mg of each sample was weighed into a vial, and an aliquot of the recovery solution (containing Terphenyl-D14 at a concentration of 1 μg/mL) was added. The sample was extracted with two separate portions of 10 mL of dichloromethane for 30 min in an ultrasonic bath, and the extract was concentrated in a rotary evaporator to 1 mL. Next, an aliquot of the internal standard solution (containing naphthalene-D8, phenanthrene-D10, chrysene-D12, and perylene-D12 at a concentration of 1 μg/mL) was added. The extract was then analyzed by gas chromatography coupled with mass spectrometry. Details of the GCMS method and instrument can be found in SI.

2.7. Inorganic compounds

Samples were sent to the Technological Characterization Laboratory (LCT, Department of Mining and Petroleum Polytechnic School – USP).

2.7.1. Scanning electron microscopy

Samples were dispersed in air on double-sided carbon tape and then metallized with carbon to be evaluated using a scanning electron microscope.

The scanning electron microscope used was the Quanta 650 FEG model (Thermo Fisher Scientific™), with EDS detectors, Bruker brand, models XFlash 4030 and XFlash 6–60; the software used to analyze was Esprit, from Bruker, version 2.3. The metalizer was the SCD-050 Coating System model, Bal-tec brand.

2.7.2. FRX – X - ray fluorescence

The inorganic composition was assessed semi-quantitatively using a Malvern Panalytical Zetium X-ray fluorescence spectrometer with STD-1 (standardless) calibration. Measurements were conducted on a pressed sample for elements from fluorine to uranium, and the values were normalized to 100 %.

2.7.3. Neutron activation analysis (NAA)

The analysis was conducted at the Research Reactor Center of the Nuclear and Energy Research Institute (IPEN), São Paulo. Samples were activated through bombardment with thermal neutrons. When a neutron collides with the nucleus of the target, a highly excited compound nucleus is formed. The de-excitation process generates gamma radiation. Elements were identified and quantified based on their characteristic gamma rays.

2.8. Cell culture

2.8.1. BEAS-2B and A549

BEAS-2B cells (Sigma Aldrich) in passages between 9 and 10 were cultured in LHC-9 culture medium (Gibco, Life Technologies) and Lung adenocarcinoma cell line (A549) cells in passages between 11 and 13 were cultured in RPMI culture medium (Lonza) supplemented with 10 % fetal bovine serum (FBS), in a humidified incubator at 37ºC with 5 % CO2. A549 was generously donated by Cancer Molecular Biology Laboratory (LBMC), Department of Biochemistry at the Institute of Chemistry – USP.

2.9. MTT assay

BEAS-2B and A549 cells were maintained in culture medium in 96-well plates at approximately 90 % confluence. DEP and APE particles were resuspended in PBS at a ratio of 1 mg:1 mL and sonicated for 15 min to improve dispersion. Particles were diluted in culture medium to 10, 50 or 100 μg/mL concentration. MTT assay (Invitrogen) was performed according to manufacturer instructions.

2.10. Peripheral blood monocytes derived macrophages (PBMC)

Blood was collected from 3 healthy individuals with no history of smoking, in sodium heparin tubes. PBMCs were density separated with HISTOPAQUE-1077 (Sigma Aldrich). Monocytes were incubated for 5 days with M-CSF (50 ng/mL, Peprotech, USA) and IL-6 (25 ng/mL, Peprotech, USA) for M2 polarization, or GM-CSF (50 ng/mL, Peprotech, USA) for M1 polarization.

2.10.1. Co-culture establishment

For the co-culture, macrophages and BEAS-2B or A549 were seeded together in 1:4 ratio, resulting in an inflammatory model. The co-culture was maintained 24 h before the exposure. After 24 h of co-culture, cells were exposed to APE and DEP at a concentration of 50 μg/mL for 24 h. Table 1 in SI summarizes the study groups.

2.11. Macrophage immunophenotyping

Viability was assessed by cytometry using the LIVE/DEAD™ Fixable Dead Cell Stain Sampler Kit (Thermo Fisher). Markers and fluorophores used were: CD14 (BV605–2.5:100, BD™) for macrophages; HLA-DR - Human Leukocyte Antigen – DR - (PE-Cy7–1:200, BD™) for M1; CD163 (Alexa 467–1:200, BD™); CD209 (PercP-Cy5.5–1:200, BD™) for M2; and FITC (0.25 μL/mL) for Live/Dead.

Samples were analyzed on the Fortessa cytometer at IMT - Institute of Tropical Medicine, collecting at least 150,000 events. Analysis was performed using Floreada.io. Independent triplicates were done for each group. Median Fluorescence Intensity (MFI) and percentage of positive cells were used to characterize the populations. MFI represents the fluorescence intensity detected in a given cell population and serves as a quantitative measure of protein expression. It is used to assess relative protein levels, as fluorescence intensity is proportional to protein abundance.

For immunophenotyping DEP exposure was excluded due to the risk of particle clogging of the cytometer system.

2.12. Cytokine assay

Cytokines were analyzed using the MILLIPLEX MAP Human Cytokine/Chemokine Magnetic Bead Panel - Immunology Multiplex Assay

Table 1
Elements in APE and DEP.

Quantitative NAA (mg/kg)			Semi-quantitative FRX		
Elements	**APE**	**DEP**	**Elements**	**APE**	**DEP**
Na	1.06 ± 0.03	0.025 ± 0.0008	Na	1,08	0,98
Mg	242 ± 37	*ND*	Mg	0,78	0,24
Ca (%)	13.1 ± 0.6	*ND*	Ca	1,19	8,93
Mn	23 ± 0.9	61 ± 1	Mn	*ND*	0,16
Cr	44 ± 2	36 ± 2	Cr	0,03	*ND*
Fe (%)	*ND*	0.102 ± 0.003	Fe	3,25	16,02
K (%)	0.07 ± 0.01	*ND*	K	1,62	1,13
Zn	280 ± 11	1544 ± 66	Zn	0,03	1,30
V	6.1 ± 0.8	1.4 ± 0.02	S	2,27	16,71
Ba	8 ± 2	*ND*	Cu	0,02	*ND*
Br	19.9 ± 0.01	0.64 ± 0.07	Al	15,19	1,11
Ce	10.5 ± 0.7	*ND*	Si	22,35	3,24
Co	0.17 ± 0.01	0.37 ± 0.02	Cl	0,97	1,35
Cs	0.11 ± 0.03	*ND*	P	1,30	2,95
			Ti	1,65	0,23
			Ni	*ND*	0,09
			As	0,04	0,27

(Merck™), in conjunction with the Luminex® xMAP® platform in a magnetic bead format. A total of three independent experiments were performed for each group described in SI Table 1, following APE or DEP exposure. Supernatants were collected, centrifuged (14,000 RPM, 10 min), and stored at −80°C for further analysis. For each test, 50 μL of sample were used. Results were normalized to the non-exposed control (CTR). The selected cytokine panel included IFN-γ, IL-10, IL-1β, IL-6, IL-8, and TNF-α.

2.13. qRT-PCR

Real-time PCR was conducted to evaluate the activation of xenobiotic metabolism (CYP1A1 and CYP1B1) and the expression of p53 and EGFR in response to APE and DEP exposure.

Total RNA was obtained using the TRIzol™ Plus RNA Purification Kit (Invitrogen™), together with DNase treatment (PureLink™ DNase Set - Invitrogen™). The total RNA was converted into complementary DNA (cDNA) using the High-Capacity cDNA Reverse Transcription Kit (Applied Biosystems™).

Pre-designed TaqMan® Gene Expression Assay (Applied Biosystems™) was used for genes described in SI Table 2. Three independent experiments were conducted for each group. Results were calculated via the ΔΔCT method.

2.14. Statistics

Statistical analyses were conducted using SigmaPlot Software (Systat Software, Inc.). PAHs quantification in APE and DEP was compared using one-way ANOVA for individual PAHs (APE vs. DEP). Two-way ANOVA was used for comparisons based on molecular weight, considering particle type (Factor A: APE vs. DEP) and molecular weight category (Factor B: low vs. high, in μg/g). Additionally, a separate two-way ANOVA was performed to compare the number of rings, with particle type (Factor A: APE vs. DEP) and ring number (Factor B: 2, 3, 4, 5, or 6). Post hoc pairwise comparisons were conducted using Tukey's test, with significance set at $p \leq 0.05$.

For biological effects, three independent experiments were conducted to assess cell viability, immunophenotyping, RT-PCR, and cytokine release. For the MTT assay, two-way ANOVA was used to analyze multiple comparisons, considering particle type (APE vs. DEP) and particle concentration (10, 50, and 100 μg/mL). Two-way ANOVA was applied for cytokine markers and mRNA fold change, considering study groups and particle type. Post hoc pairwise tests were performed using Tukey's test for cytokine release and Holm-Sidak for RT-PCR and flow cytometry, with significance set at $p \leq 0.05$. For macrophage immunophenotyping, we performed one-way ANOVA for each marker using GraphPad Prism, presenting the results as relative percentages compared to the control group. The Holm-Sidak method was used as a post hoc test, with statistical significance set at $p \leq 0.05.3$.

3. Results

Demographic information of 35 lung fragment donors is in Table 3 of Supplementary Information (SI). The median age was 73 years, with 18 males and 17 females. None had occupational exposure to coal or biomass burning products. Residency time ranged from 5 to 91 years. Of the 35 individuals, only one was a smoker (10 cigarettes per day), and 9 were former smokers, the most recent having quit a year ago. A total of 141.55 g of tissue was processed, yielding 797.3 mg of black powder from anthracotic tissue extraction and subsequent chemical analysis.

3.1. Chemical characterization reveals differences between APE and DEP composition

Table 1: Summarizes elements detected by NAA and FRX.

Neutron Activation Analysis (NAA) is a highly sensitive technique well-suited for multielement characterization of particulate matter, and it was used to quantify inorganic elements in the sample based on their gamma-energy signatures. In parallel, X-ray fluorescence (XRF) was employed, which uses X-ray-induced electronic excitation to identify inorganic compounds. Due to the rare nature of our sample, standardless XRF was applied, resulting in approximate values derived from atomic physics models. As the data were normalized to 100 %, the results represent the relative proportions of the detected elements. The same pooled anthracotic extract was analyzed using both methods, which complement each other.

Both techniques detected higher levels of Na, Mg, Cr, K, and Zn in APE, and more Fe and Mn in DEP. Table 1 shows that NAA did not quantify Mg, Ca, or K in DEP, nor Fe in APE. DEP contains about 5 times more Zn than APE, while APE has roughly 6 times more V than DEP. Mn was detected in both particles, with DEP showing nearly three times higher levels than APE. Although FRX provides semi-quantitative results, it revealed higher sulfur in DEP and more silica in APE. SEM results are shown in SI Figure 3 and 4, presenting different elements observed in APE and DEP samples. Although not quantified, elements like Fe and Si were present in APE. Calcium was detected in both particles (SI Fig.3 and 4 G) but quantified only in APE, despite higher percentages in DEP according to FRX (Table 2). The techniques aimed to comprehensively explore APE's elemental composition, but inconsistencies in particle characterization require further investigation.

3.2. DEP contains more complex PAHs than APE

Table 2 shows PAHs (Polycyclic Aromatic Hydrocarbons) species detected by gas chromatography coupled with mass spectrometry after particles decontamination. A comparison of particles before and after decontamination is in SI. Table 4.

PAHs analysis shows that DEP has 5.28 times more PAHs than APE. Also, DEP presented more PAHs of high molecular weight than APE. Fig. 1 shows graph results comparing APE and DEP considering PAHs molecular weight and number of rings.

As shown in Fig. 1A, APE contains significantly more low-molecular-weight (LMW) PAHs than high-molecular-weight (HMW) PAHs ($p < 0.001$). DEP has higher levels LMW and HMW PAHs compared to APE ($p < 0.001$). Regarding ring number (Fig. 1B), APE has more 2-ring PAHs ($p < 0.001$), while DEP has more 4- and 5-ring PAHs ($p < 0.001$).

Table 2
PAHs composition APE vs DEP.

Polycyclic Aromatic Hydrocarbons (PAHs)	Content (μg/g)	
	APE Irradiated	DEP Irradiated
Naphthalene (C10H8)	2.44 ± 0.38	5.17* ± 0.03
Acenaphthylene (C12H8)	0.47* ± 0.06	*ND*
Acenaphthene (C12H10)	*ND*	0.47 ± 0.01
Fluorene (C13H10)	0.54# ± 0.23	0.28 ± 0.01
Phenanthrene (C14H10)	0.53 ± 0.01	6.69* ± 0.02
Anthracene (C14H10)	< 0.1	*ND*
Fluoranthene (C16H10)	0.14 ± 0.01	3.12* ± 0.07
Pyrene (C16H10)	0.27 ± 0.01	3.09* ± 0.06
Benzo[*a*]anthracene (C18H12)	< 0.1	0.88* ± 0.01
Chrysene (C18H12)	< 0.1	0.81* ± 0.03
Benzo[*k*]fluoranthene (C20H12)	*ND*	0.76* ± 0.03
Benzo[*b*]fluoranthene (C20H12)	*ND*	< 0.1
Benzo[*j*]fluoranthene (C20H12)	*ND*	< 0.1
Benzo[*e*]pyrene (C20H12)	*ND*	0.55* ± 0.05
Benzo[*a*]pyrene (C20H12)	*ND*	1.21* ± 0.09
Indeno[1,2,3-cd]pyrene (C22H12)	*ND*	< 0.1
Dibenzo[*a,h*]anthracene (C22H14)	*ND*	< 0.1
Benzo[*g,h,i*]perylene (C23H14)	*ND*	< 0.1
Total PAHs	4,39	23,18

The symbol * reveals statistically significant p value of $p < 0.001$ and # for $p < 0.008$, obtained by One Way ANOVA test (p values in SI Table 5).

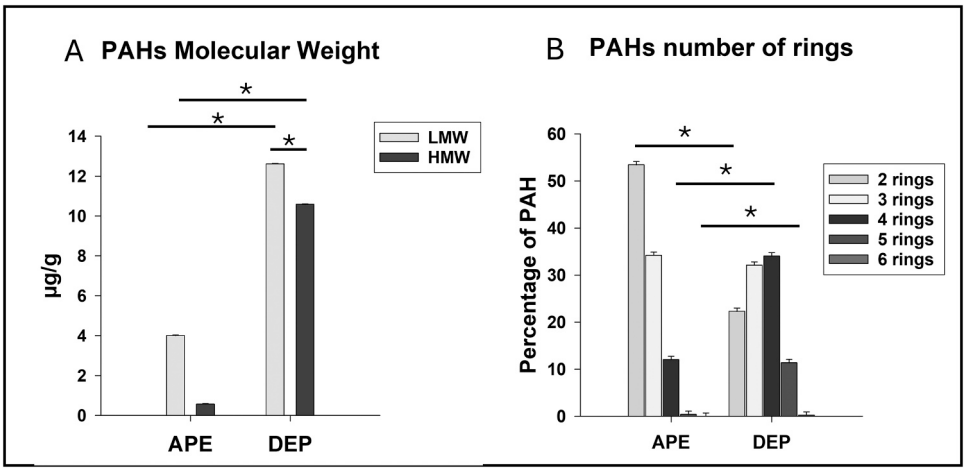

Fig. 1. PAHs characteristics in APE and DEP A) Comparison between APE and DEP considering low molecular weight LMW = low molecular weight; HMW = high molecular weight. B) PAHs in APE and DEP considering number of rings. Symbol * means $p < 0.001$ (p values in SI Table 5).

3.3. APE exposure reduces metabolism in BEAS-2B and viability of macrophages in co-culture

MTT was performed as a cytotoxicity assay in BEAS-2B and A549 cell lines. Cells were exposed to both APE and DEP for 24 h at concentrations of 10, 50 and 100 µg/mL. Fig. 2 shows relative MTT values.

BEAS-2B was more susceptible to cytotoxicity from particle exposure than A549 cell line. Cell metabolism significantly decreased in all groups of BEAS-2B ($p < 0.001$) compared to control (Fig. 2A), while in A549 only DEP at higher concentration showed a significant change ($p = 0.039$).

Live and Dead staining was performed for general cell viability. Fig. 2B shows viability results after 24 h of exposure to 50 µg/mL APE. Due to macrophage and BEAS-2B ratio in co-culture (1:4), their viability did not change when exposed to APE (Fig. 2B). However, when analyzing only CD14 + cells of co-culture (Fig. 2B), macrophage viability significantly decreased after exposure to APE ($p < 0.001$). Monocultures showed a decrease in viability when M0-APE was compared to M1-APE ($p = 0.018$), and M2-APE when compared to M2 CTR ($p = 0.044$).

DEP was excluded as a positive control in flow cytometry due to the risk of clogging the cytometer system. A549 co-cultures were also not analysed, as A549 cells express CD14 (Barbosa et al., 2007) and HLA-DR (Senosain et al., 2021), making it difficult to differentiate them from macrophages.

3.4. APE induces changes in macrophage profile both in co-culture with BEAS-2B and monoculture

For macrophage profile study, a pre-treatment of macrophages with GM-CSF (M1) and M-CSF/IL-6 (M2) was performed. Non-treated macrophages (M0) were used for comparison. After APE exposure at 50 µg/mL for 24 h, macrophages showed a heterogeneous population, expressing both M1 (Human Leukocyte Antigen – DR - HLA-DR) and M2 (CD163 and CD209) markers, as shown in Fig. 3.

After APE exposure (Fig. 3A-C), all co-cultures showed increased HLA-DR (M1 profile, $0.001 < p < 0.0067$) while M2 markers decreased ($p < 0.001$)In macrophage monocultures (Fig. 3D-F), HLA-DR increased in M0-APE ($p = 0.005$), M1-APE ($p < 0.001$), but M2 maintained lower HLA-DR expression ($p = 0.014$). CD163 was significantly lower in M2 ($p < 0.001$) after APE exposure.

These results suggest macrophage populations were heterogeneous, expressing mainly HLA-DR/CD163, and tended toward increased HLA-DR after APE exposure. Figure 5 and 6 (SI) show percentages of HLA-DR-positive and HLA-DR/CD163 co-expressing cells. In co-culture, BM0 had a mostly double-positive population in CTR (58.06 %), but after APE exposure HLA-DR expression increased (60.02 % $p < 0.001$), suggesting a shift toward a pro-inflammatory profile (Figure 5A-SI). BM1 also showed increased HLA-DR after APE exposure (57.60 % $p < 0.001$) (Figure 5B-SI), while BM2 remained predominantly double-positive (61.88 %) but with increased HLA-DR expression post-APE ($p < 0.001$) (Figure 5C-SI).

In monoculture, HLA-DR/CD163 double-positive cells were higher in M0 (57.77 % $p < 0.001$), regardless of APE exposure (Figure 6A-SI). Pre-induced macrophages responded differently: M1-APE increased HLA-DR (59.94 % $p = 0.03$), while M2-APE decreased (28.03 % $p < 0.001$) (Figure 6 B-C-SI).

Overall, APE induced a pro-inflammatory response in co-cultures, increasing HLA-DR-positive cells.

3.5. APE exposure induced increased cytokines release in co-culture and macrophages

Fig. 4 represents results of cytokine release for BEAS-2B and A549 cell lines alone or with M1 and M2 induced macrophages co-cultures.

As shown in Fig. 4A-F, BEAS-2B cell line had no significant release of any cytokine, however, when in co-culture with macrophages there was a marked increase in cytokine expression after 24 h of APE 50 µg/mL exposure. Increased IFN-ɣ, IL-10 and TNF-α are observed in BM1 ($p = 0.008$, $p = 0.009$, $p = 0.006$) and BM2 ($p = 0.036$, $p < 0.001$, $p = 0.006$) groups exposed to APE, but surprisingly DEP did not provoke changes in cytokine releasing. Similar results can be observed for AM1 showing increased IL-10 ($p = 0.011$), IL-1β ($p = 0.028$) and IL-6 ($p = 0.003$) after APE exposure, and AM2 increasing IFN-ɣ ($p = 0.019$), IL-10 ($p = 0.001$) and TNF-α ($p = 0.022$), also after APE exposure, while DEP showed no increase in cytokine. In addition, macrophages in monoculture showed increased cytokine release in response to APE exposure (Figure 7 SI).Those results suggest that only APE is capable of sensitizing epithelial cells and only in the presence of macrophages.

3.6. APE exposure did not change P450 enzymes expression

Results for mRNA expression of P450 enzymes, p53 and EGFR are represented in Fig. 5.

As was expected, DEP significantly increased CYP1A1 and CYP1B1 expression in BEAS-2B ($p < 0.001$) and co-cultures BM1 ($p = 0.007$) and BM2 ($p = 0.021$); and A549 ($p = 0.001$) and co-cultures AM1 ($p = 0.002$) and AM2 ($p = 0.02$) (Fig. 5A-B and E-F). CYP1A1 has a mRNA fold change of 8 for BEAS-2B groups (Figs. 5A) and 4 for A549

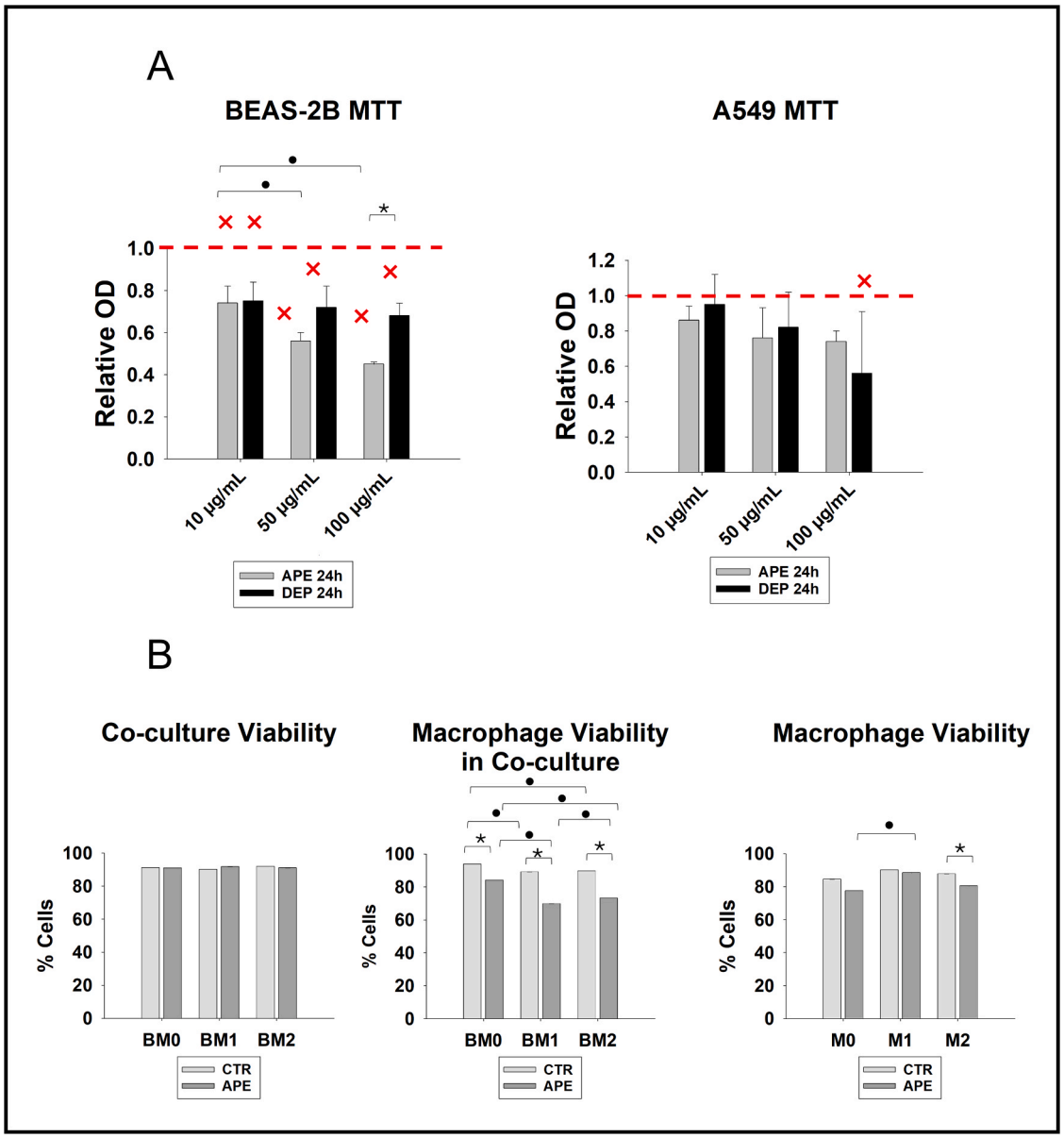

Fig. 2. Cell metabolism and viability A) Cell metabolism accessed by MTT assay in BEAS-2B and A549 co-culture exposed to APE or DEP for 24 h. Red dashed means CTR = 1, the • symbol means significant values between concentrations (10 vs 50 vs 100), the * symbol means significant values between APE and DEP groups and red × symbol means significant values comparing to control (p values in SI table 6) B) Cell viability evaluated using the Live/Dead assay by flow cytometry, including both co-cultures and monocultures. The • symbol means significant values between culture groups, * symbol means significant values between CTR and APE groups (p values in SI table 7).

groups (Fig. 5E), indicating that DEP caused an upregulation of P450 enzymes. However, APE exposure did not change xenobiotic enzymes expression.

Regarding p53, BM1-APE presented lower expression compared to BM1-DEP ($p = 0.029$), BEAS-2B-APE ($p = 0.002$) and BM2-APE ($p = 0.01$) (Fig. 5C). AM1-APE had a decreased p53 expression when compared to AM1-DEP ($p = 0.01$), AM1-CTR (0.017) and A549-APE ($p = 0.01$) (Fig. 5E). Therefore, M1 co-cultures exposed to APE generally showed downregulation of p53. However, AM2-DEP showed an increase in p53 when compared to A549-DEP ($p = 0.025$). Considering EGFR expression, BM1-DEP ($p = 0.024$) and BM2-DEP ($p = 0.035$) had increased expression when compared to BEAS-2B-DEP, suggesting that DEP may induce cell proliferation when BEAS-2B and macrophage are together. AM2-APE ($p = 0.003$) had increased EGFR expression when compared to AM2- CTR and to A549 groups ($p = 0.009$), suggesting that DEP may induce cell proliferation when adenocarcinoma cells and M2-like macrophage are together as well.

4. Discussion

In this study, we have shown that anthrachotic particles retained in the lung have harmful effect on co-culture of bronchial epithelial cells (BEAS-2B) or A549 lung adenocarcinoma cells and M0, M1 and M2 macrophages by inducing inflammatory cytokine release and modulating macrophages behavior.

To our knowledge, this is the first study to present a technique allowing the extraction of anthracotic material from the lung and its subsequent use in *in vitro* tests. A limitation of this newly proposed technique is the lack of controls for particle extraction. However, preliminary tests showed no decrease in cell viability when assessing Corolase residues, and pilot results for PAH characterization were consistent. Since this method was applied for the first time, future

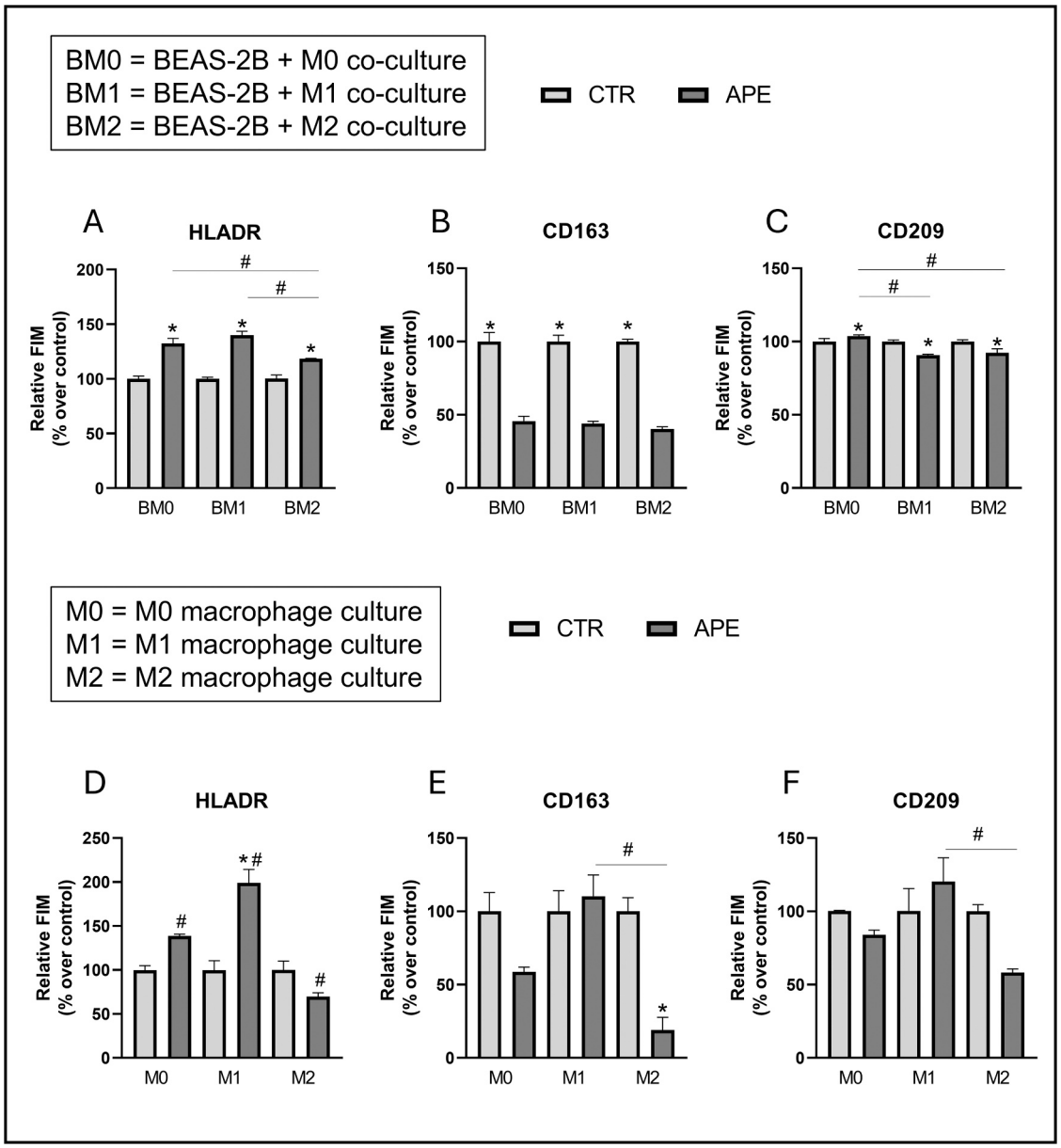

Fig. 3. Relative fluorescence intensity median (FIM) over the unexposed group (CTR) A) HLA-DR in co-culture with BEAS-2B and macrophages; B) CD163 in co-culture with BEAS-2B and macrophages; C) CD209 in co-culture with BEAS-2B and macrophages; D) HLA-DR in monoculture macrophages; E) CD163 in monoculture macrophages; F) CD209 in monoculture macrophages. The # indicates significant differences between culture groups; the * indicates significant differences between CTR and APE groups (p-values in SI Table 8).

refinements in the extraction protocol can address this gap.

The chemical composition of particulate matter from anthracotic tissue and diesel exhaust particles was different. DEP was chosen as a positive control because during its collection there were no reactions with atmospheric substances or biological interactions, the opposite of APE. Metals in DEP are usually associated with lube oil (e.g., Zn, Fe, Ca, Al, Mg, Cu and Cr) and fuel additives (e.g., Zn, Fe, Ca, Al, Mg, Ni, V, Si, and Na) (Martins et al., 2021; Rana et al., 2022). Despite the inorganic composition of both APE and DEP sharing common characteristics (Tables 1–2), DEP contained higher levels of PAHs with greater molecular weight, as well as more iron, manganese, zinc, and sulfur—findings that are consistent with previous characterizations of particles of this nature (Nan et al., 2023; Cui et al., 2022; Zerboni et al., 2022).

As expected, DEP had in its composition more PAHs of higher molecular weight and more iron, manganese, zinc and sulfur, which corroborates other characterizations of particles of this nature (Cui et al., 2022; Zerboni et al., 2022) Anthracosis derived particulate presented significantly more PAHs of two carbon rings and greater amounts of calcium, vanadium, bromine and magnesium. These differences in particle composition may have been important for the difference found in cultures and co-cultures responses to exposure.

The differences in the amount of metals, PAHs, and the nature of these PAHs found in APE compared to DEP were expected – likely resulting from biological metabolization – and support the representative nature of our extract. It is known that high molecular weight PAHs are harmful to different cell types but have a lower tendency to bioaccumulate (Jin et al., 2021; Glencross et al., 2020). After entering the body through inhalation, particulate matter can be retained in the upper respiratory tract, where mucociliary clearance helps expel a large portion of the particles (Clarà et al., 2023). However, ultrafine particles may reach and persist in the deeper regions of the respiratory system, where macrophages engulf some of them and tissue cells attempt to

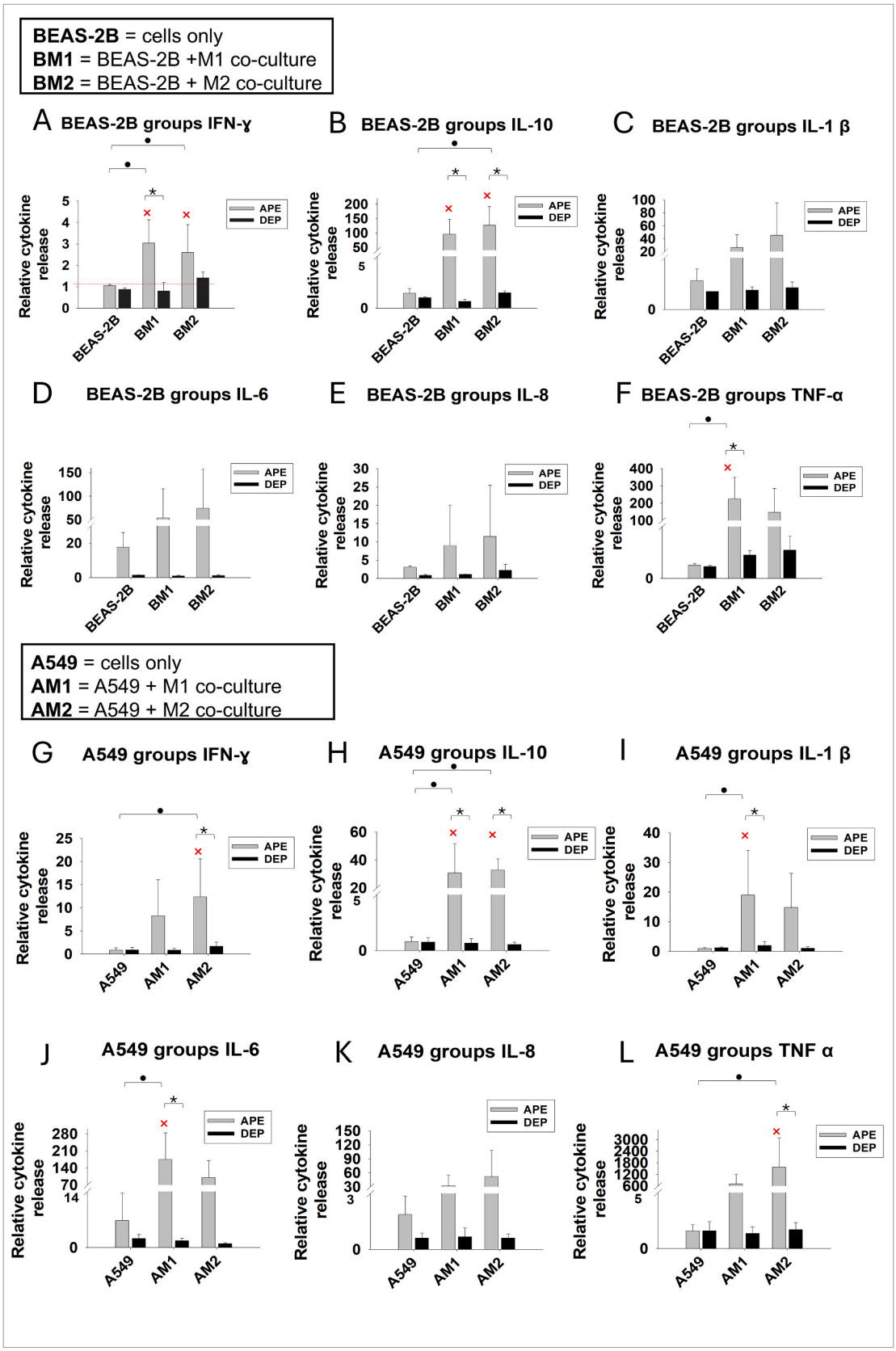

Fig. 4. Cytokine panel for IFN-ɣ, IL-10, IL-1 β, IL-6, IL-8 and TNF α expression. Cytokine levels were measured in cell culture supernatants (pg/mL) and normalized to the control group. A-F) BEAS-2B groups; G-L) A549 groups. Red dashed means CTR = 1, the • symbol means significant values between culture groups, the * symbol means significant values between CTR and APE groups and red × symbol means significant values compared to control (p values in SI Table 10).

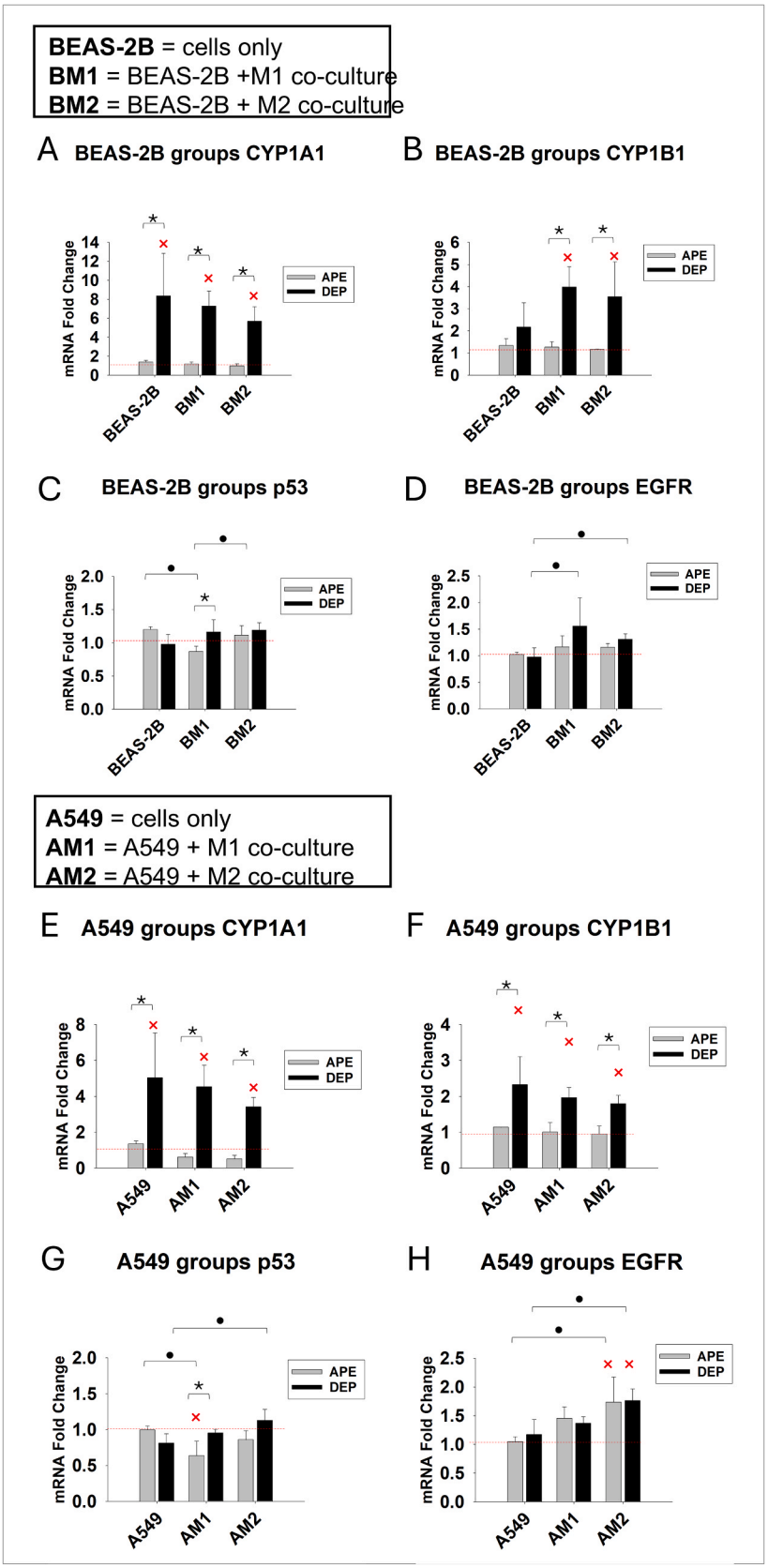

Fig. 5. RT-PCR results for CYP1A1, CYP1B1, p53, and EGFR mRNA expression after 24 h of APE or DEP exposure (50 μg/mL). A) CYP1A1 expression in BEAS-2B, BM1, and BM2; B) CYP1B1 expression in BEAS-2B, BM1, and BM2; C) p53 expression in BEAS-2B, BM1, and BM2; D) EGFR expression in BEAS-2B, BM1, and BM2; E) CYP1A1 expression in A549, AM1, and AM2; F) CYP1B1 expression in A549, AM1, and AM2; G) p53 expression in A549, AM1, and AM2; H) EGFR expression in A549, AM1, and AM2. Red dashed line indicates CTR = 1; • indicates significant differences between culture groups; * indicates significant differences between CTR and APE groups; red × indicates significant differences compared to control (p-values in SI Table 12).

chemically neutralize their compounds (Bai et al., 2018). Since metals and PAHs are among the most common substances adsorbed onto urban particulate matter, antioxidant enzymes are activated to mitigate oxidative stress – primarily caused by metals – while the aryl hydrocarbon receptor (AhR) induces CYP450 enzymes to metabolize PAHs (Moorthy et al., 2015; Shimada and Fujii-Kuriyama, 2004; Wāng, 2025).

Cytochrome P_{450} enzymes are responsible for metabolize xenobiotics in cells, mainly PAHs, and represents a common response in models exposed to atmospheric particulate matter (Moorthy et al., 2015; Glencross et al., 2020). Our results show that DEP contains approximately five times more PAHs than APE, that may have contributed to the increased CYP expression, but it was intriguing that cytokine release was so lower than APE. As a possible explanation, the aryl hydrocarbon receptor (AhR) has been reported to partially modulate the release of inflammatory cytokines in pulmonary cells exposed to particulate matter (Grytting et al., 2025; Jaguin et al., 2015; Rothhammer and Quintana, 2019; O'Driscoll et al., 2018). Other studies have demonstrated AhR's role as a negative regulator of inflammation in lung cell lines (Grytting et al., 2025; Vázquez-Gómez et al., 2022). Therefore, it is possible that AhR activation following DEP exposure may modulate cytokine release, resulting in lower levels of inflammatory markers. However, the mechanisms involved in this pathway, and the threshold of cellular stress required to activate it, remain unclear.

On the other hand, APE presented a lower amount and simpler structure of PAHs compared to DEP. Low molecular weight PAHs are often considered less harmful than high molecular weight', but it is known that they can increase inflammatory responses in macrophages (Wang et al., 2017; Bright et al., 2023), while inhibiting CYPs expression (Wang et al., 2017). The interactions between inflammatory cytokines and CYPs expression might be complex and there are studies reporting an inverse relationship between CYPs expression and pro-inflammatory cytokines, like TNF-α and IL-6 (Aitken and Morgan, 2007; Frye et al., 2002). Also, TNF-α appears to have a role in modulating AhR target genes in epithelial cells exposed to fluoranthene (Kabátková et al., 2015). In this study, APE exposure modulated macrophage profile to pro-inflammatory-like and increased TNF-α release in co-culture's supernatant, which may have induced an immune response that could downregulate P_{450} activation. However, the mechanistic pathway underlying this response warrants further investigation.

Considering significant amounts of inflammatory cytokines released in co-cultures after APE exposure, such as TNF-α, IL-6, IFN-ɣ and IL-1β (Fig. 4), it can be inferred that APE was more immunogenic than DEP. Both BEAS-2B and A549 alone had no significant change in cytokine release, increasing only when these cells are in culture with pre-induced macrophages. In normal epithelial cells (BEAS-2B), exposure to particles led to a significant decrease in metabolism, while only the highest concentration of DEP disrupted A549 metabolism. Although immortalized, these cell lines likely retain characteristics of their original tissues. Adenocarcinoma cells subvert survival mechanisms (Chen et al., 2020) and are genetically unstable (Park et al., 2001), which would explain this difference in susceptibility to damage caused by APE and DEP in monocultures.

Despite M1 is considered a pro-inflammatory phenotype and M2 is considered an immunosuppressive phenotype (Najafi et al., 2019), macrophages are plastic cells and the M1/M2 dichotomy has been questioned over the years, leading to an understanding that there is a spectrum of macrophage activation between these two extremes, considering that their profile/behavior will depend on the microenvironment stimuli and pathological conditions (Ruytinx et al., 2018; Martinez and Gordon, 2014; Wang et al., 2020a). As shown in Figure SI-6, the apparent decrease in the HLA-DR marker in M0 monoculture was accompanied by an increase in cells co-expressing HLA-DR and CD163, indicating a more heterogeneous population compared to co-cultured macrophages.

In co-culture, macrophage behavior could be influenced by pulmonary cells (Zhou et al., 2022). In this study, when co-cultured with bronchial-derived cells and exposed to particles, macrophages acted as "inflammatory recruiters", showing a stronger M1-like profile and releasing pro-inflammatory cytokines. In contrast, in monoculture, macrophages were influenced solely by the particles, which triggered both inflammatory markers and tissue repair mechanisms, leading to a balanced expression of M1- and M2-associated profiles.

In cell viability results for BEAS-2B and macrophages co-culture, APE reduced the viability of macrophages in relation to control (Fig. 4B). Under an inverted microscope, it was possible to perceive phagocytic activity in co-cultures (Figure 8 SI) exposed to both particles, which may have influenced the viability of macrophages, consequently influencing the release of cytokines and CYPs response.

The expression of p53 and EGFR genes, both involved in cell cycle regulation, was altered after particle exposure. The p53 gene plays a key role in cell cycle checkpoints, preventing DNA replication errors and tumor development (Stading et al., 2021; Bennett et al., 1999). Previous studies have shown that PM2.5 exposure can upregulate p53 (Jin et al., 2023; Cheng et al., 2024) and induce senescence in alveolar cells and lung fibroblasts, while also promoting lung carcinogenicity by increasing IL-17a and downregulating p53 in mice (Chao et al., 2020). However, the modulation of p53 by immune responses following PM exposure remains unclear. In our study, APE exposure led to decreased p53 expression in BM1 cells, alongside increased HLA-DR-positive cells and elevated INF-γ and TNF-α levels, suggesting that interactions between BEAS-2B and pro-inflammatory macrophages may contribute to p53 downregulation.

A549 tumor cells also showed changes in p53 and EGFR expression: AM1 cells decreased p53 after APE exposure, while AM2 cells increased EGFR expression after both APE and DEP exposure. These changes were accompanied by increased cytokine release in AM1 and AM2, which may have influenced EGFR expression, as oxidative stress from PM exposure is known to promote cytokine release via EGFR activation (Wang et al., 2020b). In contrast, DEP exposure did not increase cytokine release, suggesting that its complex composition may directly affect EGFR expression. Notably, high molecular weight PAHs such as benzo (a)pyrene have been shown to promote A549 proliferation via EGFR phosphorylation (Kometani et al., 2009). Additionally, co-culture with macrophages may have influenced cell behavior, as vesicle-mediated communication between A549 cells and macrophages has been demonstrated in vitro (Pritchard et al., 2020).

Although malignant lesions associated with anthracosis have been rarely reported and no strong epidemiological link has been established between anthracosis and lung cancer, individuals with anthracosis may be more susceptible to cancer development and poor prognosis (Defaee et al., 2025). In vivo models are usually more suitable for investigating complex tumor behavior, as inflammatory processes within the tumor microenvironment – triggered by air pollutant exposure – may contribute to tumor progression (Riva et al., 2020; Hill et al., 2023). However, in vitro studies can offer valuable insights into the mechanisms underlying this progression.

Due to the pooling of extracts, it was not possible to perform a correlation analysis between donor demographics and the composition of APE. Of the 35 cases collected, 21 had cardiopulmonary conditions related to their causes of death. Limitations of the study include potential exposure to particulate matter from other sources, such as cigarette smoke or occupational activities. It is also possible that biological residues from the extraction process contributed to the inflammatory-like response observed in the co-culture model. However, since environmental particles naturally contain biological components - just as the tissue environment does - the interaction of these elements with the particles may, to some extent, mimic physiological conditions, particularly in inflammatory scenarios. Despite the limitations related to extraction, this material appears to reflect the characteristics of particulate matter retained in tissue after undergoing biological transformations, thereby offering a valuable perspective on what our respiratory system is chronically exposed to in daily life.

The findings suggest a progression of damage from polluted air inhalation over time. DEP, rich in PAHs, strongly activates AhR, triggering xenobiotic metabolism and a moderated inflammatory response. In contrast, APE – with lower PAH content – may weakly activate AhR, failing to suppress inflammation and leading to elevated cytokine release. This implies that initial particle exposure activates detox pathways, while prolonged presence and transformation shift the response toward inflammation. Thus, the respiratory system is likely subjected to both processes simultaneously and chronically, especially in urban populations like those in São Paulo.

5. Conclusions

In conclusion, the extraction of particulate matter from anthracotic tissue in autopsied lungs was successful, enabling direct *in vitro* cell exposure. The anthracotic tissue derived particles differ chemically from diesel exhaust particulates, containing low-molecular-weight PAHs with up to two rings. APE and DEP induced different responses in lung cells and macrophages, likely due to their chemical composition. APE triggered pro-inflammatory cytokine release but did not affect xenobiotic metabolism, while DEP increased xenobiotic metabolism without promoting cytokine release. The complex immune modulation pathway through AhR may explain the differing responses in monocultures and co-cultures.

Funding

This work was supported by Coordination of Higher Education Personnel Improvement – CAPES and the São Paulo Research Foundation – FAPESP (grant numbers 2019/03586–2 and 2018/23975–0).

CRediT authorship contribution statement

Regiani Carvalho-Oliveira: Writing – review & editing. **Fábio Vitório Sussa:** Investigation. **Cardoso da Silva Paulo Sérgio:** Writing – review & editing. **Amorim de Lacerda João Paulo:** Writing – review & editing, Investigation. **Juliana Smelan:** Writing – review & editing, Investigation. **Gabriela Lima Vieira:** Writing – review & editing, Investigation, Formal analysis, Data curation. **Daniela Perroni Frias:** Writing – review & editing, Writing – original draft, Visualization, Validation, Project administration, Methodology, Investigation, Funding acquisition, Formal analysis, Data curation, Conceptualization. **Mariangela Macchione:** Writing – review & editing, Writing – original draft, Visualization, Validation, Supervision, Project administration, Investigation, Funding acquisition, Formal analysis, Conceptualization. **Thais Mauad:** Writing – review & editing. **Paulo Hilário Nascimento Saldiva:** Writing – review & editing.

Declaration of Competing Interest

The authors declare the following financial interests/personal relationships which may be considered as potential competing interests: Daniela Perroni Frias reports financial support was provided by State of Sao Paulo Research Foundation. Daniela Perroni Frias reports financial support was provided by Coordination of Higher Education Personnel Improvement. Mariangela Macchione reports financial support was provided by State of Sao Paulo Research Foundation. If there are other authors, they declare that they have no known competing financial interests or personal relationships that could have appeared to influence the work reported in this paper.

Acknowledgements

na

Appendix A. Supporting information

Supplementary data associated with this article can be found in the online version at doi:10.1016/j.tox.2025.154299.

Data availability

Data will be made available on request.

References

Aitken, A.E., Morgan, E.T., 2007. Gene-specific effects of inflammatory cytokines on cytochrome P450 2C, 2B6 and 3A4 mRNA levels in human hepatocytes. Drug Metab. Dispos. 35 (9), 1687–1693 (Sep).

Bai, Y., Bové, H., Nawrot, T.S., Nemery, B., 2018. Carbon load in airway macrophages as a biomarker of exposure to particulate air pollution; a longitudinal study of an international panel. Part Fibre Toxicol. 15 (1) (Dec).

Barbosa, F.M., Fonseca, F.L., Figueiredo, R.T., Bozza, M.T., Casadevall, A., Nimrichter, L., et al., 2007. Binding of glucuronoxylomannan to the CD14 receptor in human A549 alveolar cells induces interleukin-8 production. Clin. Vaccin. Immunol. 14 (1), 94–98 (Jan).

Bennett, W.P., Hussain, S.P., Vahakangas, Kirsi H., Khan, M.A., Shields, P.G., Harris, C.C., 1999. Molecular epidemiology of human cancer risk: gene-environment interactions andp53 mutation spectrum in human lung cancer. J. Pathol. 187 (1), 8–18 (Jan).

Boonsarngsuk, V., Suwatanapongched, T., Rochanawutanon, M., 2009. Bronchial anthracostenosis with mediastinal fibrosis associated with long-term wood-smoke exposure. Respirology 14 (7), 1060–1063. Sep.

Bright, A., Li, F., Movahed, M., Shi, Hang, Xue, B., 2023. Chronic exposure to low-molecular-weight polycyclic aromatic hydrocarbons promotes lipid accumulation and metabolic inflammation. Biomolecules 13 (2), 196. Jan.

Chao, X., Yi, L., Lan, L.L., Wei, H.Y., Wei, D., 2020. Long-term PM2.5 exposure increases the risk of non-small cell lung cancer (NSCLC) progression by enhancing interleukin-17a (IL-17a)-regulated proliferation and metastasis. Aging (Albany NY) 12 (12), 11579–11602. Jun.

Chen, D., Wu, Y.X., Qiu, Y.B., Wan, B.B., Liu, G., Chen, J.L., et al., 2020. Hyperoside suppresses hypoxia-induced A549 survival and proliferation through ferrous accumulation via AMPK/HO-1 axis. Phytomedicine 67 (153138), 153138 (Feb.

Cheng, P., Chen, Y., Wang, J., Han, Ziyu, Hao, D., Li, Y., Feng, F., et al., 2024. PM2.5 induces a senescent state in mouse AT2 cells. Environ. Pollut. 347 (123686), 123686 (Apr).

Clarà, P.C., Jerez, F.R., Ramírez, J.B., González, C.M., 2023. Deposition and clinical impact of inhaled particles in the lung. Arch. Bronc.. 59 (6), 377–382. Jun.

Cui, Y., Huang, L., Huo, T., Dong, F., Wang, G., Zhang, Q., 2019. Man-made mineral fiber effects on the expression of anti-oncogenes P53 and P16 and oncogenes C-JUN and C-FOS in the lung tissue of wistar rats. Toxicol. Ind. Health 35 (6), 431–444. Jun.

Cui, L., Ni, H., Lei, K., Gao, X., Wang, X., Liu, Z., 2022. Chemical characteristics analysis of automobile exhaust particles and the method for evaluating its ecological effect. Chemosphere 307 (136152), 136152 (Nov.

Darquenne, C., 2020. Deposition mechanisms. J. Aerosol Med. Pulm. Drug Deliv. 33 (4), 181–185. Aug.

Defaee S., Khajavi-Mayvan F., Sheybani-Arani M., Montazeri M., Barahimi E., Salimi Asl A. Anthracosis, epidemiology, gene and cancer: An updated mini-review. babol-caspjim [Internet]. 2025 Jan 1;16(1):20–7. Available from: ⟨http://caspjim.com/article-1-3903-en.html⟩.

Frias, D.P., Gomes, R.L.N., Yoshizaki, K., et al., 2020. Nrf2 positively regulates autophagy antioxidant response in human bronchial epithelial cells exposed to diesel exhaust particles. Sci. Rep. 10, 3704. https://doi.org/10.1038/s41598-020-59930-3.

Frye, R.F., Schneider, V.M., Frye, C.S., Feldman, A.M., 2002. Plasma levels of TNF-α and IL-6 are inversely related to cytochrome P450-dependent drug metabolism in patients with congestive heart failure. J. Card. Fail 8 (5), 315–319 (Oct).

Glencross, D.A., Ho, T.R., Camiña, N., Hawrylowicz, C.M., Pfeffer, P.E., 2020. Air pollution and its effects on the immune system. Free Radic. Biol. Med. 151, 56–68 (May).

Grytting, V.S., Kirkerød, E., Skuland, T., Refsnes, M., Låg, M., Sadiktsis, I., et al., 2025. Pro-inflammatory effects of road wear particles and diesel exhaust particles in bronchial epithelial cells and macrophages. Environ. Res. 283. Oct 15.

Hamanaka R.B., Mutlu G.M. Particulate matter air pollution: Effects on the cardiovascular system. Front Endocrinol (Lausanne). 2018 Nov;9(680).

Hill, W., Lim, E.L., Weeden, C.E., Lee, C., Augustine, M., Chen, K., et al., 2023. Lung adenocarcinoma promotion by air pollutants. Nature 616 (7955), 159–167 (Apr).

Hou, F., Xiao, K., Tang, L., Xie, L., 2021. Diversity of macrophages in lung homeostasis and diseases. Front. Immunol. 12, 753940 (Sep).

Hu, X., Li, Q., Shao, S., Zeng, Q., Jiang, S., Wu, Q., et al., 2017. Potential lung carcinogenicity induced by chronic exposure to PM2.5 in the rat. Environ. Sci. Pollut. Res. Int. 24 (23), 18991–19000 (Aug).

Jaguin, M., Fardel, O., Lecureur, V., 2015. Exposure to diesel exhaust particle extracts (DEPe) impairs some polarization markers and functions of human macrophages through activation of AhR and Nrf2. PLoS One 10 (2), e0116560 (Feb).

Jamaati, H., Bahrami, N., Tabarsi, P., Khosravi, A., Kiani, A., Abedini, A., et al., 2017b. Multi-Gene expression in anthracosis of the lungs as one of the risk factors for Non-Small cell lung cancer. Asian Pac. J. Cancer Prev. [Internet] 18 (11), 3129–3133. ⟨https://journal.waocp.org/article_51948.html⟩ (Available from).

Jamaati, H., Sharifi, A., Mirenayat, M.S., Mirsadraee, M., Amoli, K., Heidarnazhad, H., et al., 2017a. What do we know about anthracofibrosis? A literature review. Tanaffos 16 (3), 175–189.
Jin, X., Hua, Q., Liu, Y., Wu, Z., Xu, D., Ren, Q., et al., 2021. Organ and tissue-specific distribution of selected polycyclic aromatic hydrocarbons (PAHs) in ApoE-KO mouse. Environ. Pollut. 286 (117219), 117219 (Oct).
Jin, S., Yoon, S.J., Jung, N.Y., Lee, Wang Sik, Jeong, J., Park, Y.J., Kim, W., et al., 2023. Antioxidants prevent particulate matter-induced senescence of lung fibroblasts. Heliyon 9 (3), e14179 (Mar).
Kabátková, M., Svobodová, J., Pěnčíková, Kateřina, Mohatad, D.S., Šmerdová, L., Kozubík, Alois, Machala, M., Vondráček, J., 2015. Interactive effects of inflammatory cytokine and abundant low-molecular-weight PAHs on inhibition of gap junctional intercellular communication, disruption of cell proliferation control, and the AhR-dependent transcription. Toxicol. Lett. 232 (1), 113–121 (Jan).
Kampa, M., Castanas, E., 2008. Human health effects of air pollution. Environ. Pollut. 151 (2), 362–367 (Jan).
Kim, Y.J., Jung, C.Y., Shin, H.W., Lee, B.K., 2009. Biomass smoke induced bronchial anthracofibrosis: presenting features and clinical course. Respir. Med. 103 (5), 757–765 (May).
Klotz, O., 1914. Pulmonary anthracosis —a community disease. Am. J. Public Health (N. Y.) 4 (10), 887–916 (Oct).
Kometani, T., Yoshino, I., Miura, N., Okazaki, H., Ohba, T., Takenaka, T., et al., 2009. Benzo[a]pyrene promotes proliferation of human lung cancer cells by accelerating the epidermal growth factor receptor signaling pathway. Cancer Lett. 278 (1), 27–33 (Jun).
Kulkarni, N., Pierse, N., Rushton, L., Grigg, J., 2006. Carbon in airway macrophages and lung function in children. N. Engl. J. Med. 355 (1), 21–30 (Jul).
Leikauf, G.D., Kim, S.H., Jang, A.S., 2020. Mechanisms of ultrafine particle-induced respiratory health effects. Exp. Mol. Med. 52 (3), 329–337 (Mar).
Martinez, F.O., Gordon, S., 2014. The M1 and M2 paradigm of macrophage activation: time for reassessment. F1000Prime Rep. 6 (Mar).
Martins, V., Correia, C., Cunha-Lopes, I., Faria, T., Diapouli, E., Manousakas, M.I., et al., 2021. Chemical characterisation of particulate matter in urban transport modes. J. Environ. Sci. (China) 100, 51–61 (Feb).
Mirsadraee, M., 2014. Anthracosis of the lungs: etiology, clinical manifestations and diagnosis: a review. Tanaffos 13 (4), 1–13.
Moorthy, B., Chu, C., Carlin, D.J., 2015. Polycyclic aromatic hydrocarbons: from metabolism to lung cancer. Toxicol. Sci. 145 (1), 5–15 (May).
Najafi, M., Hashemi Goradel, N., Farhood, Bagher, Salehi, E., Nashtaei, M.S., Khanlarkhani, N., Khezri, Z., et al., 2019. Macrophage polarity in cancer: a review. J. Cell. Biochem. 120 (3), 2756–2765 (Mar).
Nan, N., Yan, Z., Zhang, Y., Chen, R., Qin, G., Sang, N., 2023. Overview of PM2.5 and health outcomes: focusing on components, sources, and pollutant mixture co-exposure. Chemosphere 323 (138181), 138181 (May).
Nguyen, H., Morgan, D.A.F., Forwood, M.R., 2007. Sterilization of allograft bone: is 25 kgy the gold standard for gamma irradiation? Cell Tissue Bank 8 (2), 81–91 (Jun).
O'Driscoll, C.A., Gallo, M.E., Hoffmann, E.J., Fechner, J.H., Schauer, J.J., Bradfield, C.A., Mezrich, J.D., 2018. Polycyclic aromatic hydrocarbons (PAHs) present in ambient urban dust drive proinflammatory T cell and dendritic cell responses via the aryl hydrocarbon receptor (AHR) in vitro. PLoS One 13 (12), e0209690. https://doi.org/10.1371/journal.pone.0209690. PMID: 30576387; PMCID: PMC6303068.
Park, S.Y., Choi, H.C., Chun, Y.H., Kim, H., Park, S.H., 2001. Characterization of chromosomal aberrations in lung cancer cell lines by cross-species color banding. Cancer Genet. Cytogenet. 124 (1), 62–70 (Jan).
Pritchard, A., Tousif, S., Wang, Y., Hough, K., Khan, S., Strenkowski, J., et al., 2020. Lung tumor cell-derived exosomes promote M2 macrophage polarization. Cells 9 (5), 1303 (May).
Rana, S., Saxena, M.R., Maurya, R.K., 2022. A review on morphology, nanostructure, chemical composition, and number concentration of diesel particulate emissions. Environ. Sci. Pollut. Res. Int. 29 (11), 15432–15489 (Mar).
Riva, L., Pandiri, A.R., Li, Y.R., Droop, A., Hewinson, J., Quail, M.A., et al., 2020. The mutational signature profile of known and suspected human carcinogens in mice. Nat. Genet. 52 (11), 1189–1197 (Nov).
Rothhammer, V., Quintana, F.J., 2019. The aryl hydrocarbon receptor: an environmental sensor integrating immune responses in health and disease. Nat. Rev. Immunol. 19 (3), 184–197 (Mar).
Ruytinx, P., Proost, P., Van Damme, J., Struyf, S., 2018. Chemokine-induced macrophage polarization in inflammatory conditions. Front. Immunol. 9 (1930) (Sep).
Senosain, M.F., Zou, Y., Novitskaya, Tatiana, Vasiukov, G., Balar, A.B., Rowe, D.J., Doxie, D.B., et al., 2021. HLA-DR cancer cells expression correlates with t cell infiltration and is enriched in lung adenocarcinoma with indolent behavior. Sci. Rep. 11 (1) (Jul).
Shimada, T., Fujii-Kuriyama, Y., 2004. Metabolic activation of polycyclic aromatic hydrocarbons to carcinogens by cytochromes P450 1A1 and 1B1. Cancer Sci. 95, 1–6.
Souza, M.B., Saldiva, P.H., Pope 3rd, C.A., Capelozzi, V.L., 1998. Respiratory changes due to long-term exposure to urban levels of air pollution: a histopathologic study in humans. Chest 113 (5), 1312–1318. https://doi.org/10.1378/chest.113.5.1312. PMID: 9596312.
Stading, R., Gastelum, G., Chu, C., Jiang, W., Moorthy, B., 2021. Molecular mechanisms of pulmonary carcinogenesis by polycyclic aromatic hydrocarbons (PAHs): implications for human lung cancer. Semin Cancer Biol. 76, 3–16 (Nov).
Takano, A.P.C., Justo, L.T., dos Santos, N.V., Marquezini, M.V., de André, P.A., da Rocha, F.M.M., et al., 2019. Pleural anthracosis as an indicator of lifetime exposure to urban air pollution: an autopsy-based study in sao paulo. Environ. Res. 173, 23–32 (Jun).
Törün, T., Güngör, G., Ozmen, İ., Maden, E., Bolukbasi, Y., Tahaoglu, K., 2007. Bronchial anthracostenosis in patients exposed to biomass smoke. Turk. Respir. J. 8, 48–51.
Valavanidis, A., Fiotakis, K., Vlachogianni, T., 2008. Airborne particulate matter and human health: toxicological assessment and importance of size and composition of particles for oxidative damage and carcinogenic mechanisms. J. Environ. Sci. Health C. Environ. Carcinog. Ecotoxicol. Rev. 26 (4), 339–362 (Dec).
Vázquez-Gómez, G., Karasová, M., Tylichová, Z., Kabátková, M., Hampl, A., Matthews, Jason, Neča, J., et al., 2022. Aryl hydrocarbon receptor (AhR) limits the inflammatory responses in human lung adenocarcinoma A549 cells via interference with NF-κB signaling. Cells 11 (4), 707 (Feb).
Wang, J.X., Choi, S.Y.C., Niu, X., Kang, Ning, Xue, H., Killam, J., Wang, Y., 2020a. Lactic acid and an acidic tumor microenvironment suppress anticancer immunity. Int. J. Mol. Sci. 21 (21), 8363 (Nov).
Wang, D., Minami, Y., Shu, Y., Konno, S., Iijima, T., Morishita, Y., et al., 2003. The implication of background anthracosis in the development and progression of pulmonary adenocarcinoma. Cancer Sci. 94 (8), 707–711 (Aug).
Wang, C., Yang, J., Zhu, L., Yan, L., Lu, D., Zhang, Q., et al., 2017. Never deem lightly the "less harmful" low-molecular-weight PAH, NPAH, and OPAH — disturbance of the immune response at real environmental levels. Chemosphere 168, 568–577 (Feb).
Wang, G., Zhang, G., Gao, X., Zhang, Y., Fan, W., Jiang, J., et al., 2020b. Oxidative stress-mediated epidermal growth factor receptor activation regulates PM2.5-induced over-secretion of pro-inflammatory mediators from human bronchial epithelial cells. Biochim. Biophys. Acta Gen. Subj. 1864 (10), 129672 (Oct).
Wäng, Y., 2025. Ambient fine particulate matter provokes multiple modalities of cell death via perturbation of subcellular structures. In: Environment International, 195. Elsevier Ltd.
Watson, A.Y., Bates, D., 1988. Biological disposition of airborne particles: basic principles and application to vehicular emissions. In Air Pollution, the Automobile, and Public Health. National Academies Press, Washington (DC; US.
Zerboni, A., Rossi, T., Bengalli, R., Catelani, T., Rizzi, C., Priola, M., et al., 2022. Diesel exhaust particulate emissions and in vitro toxicity from euro 3 and euro 6 vehicles. Environ. Pollut. 297 (118767), 118767 (Mar).
Zhou, J., Zou, H., Liu, Y., Chen, Y., Du, Y., Liu, J., et al., 2022. Acute cytotoxicity test of PM2.5, NNK and BPDE in human normal bronchial epithelial cells: a comparison of a co-culture model containing macrophages and a mono-culture model. Toxicol. Vitr. 85. Dec 1.